THE JOURNAL OF PHYSICAL CHEMISTRY Letters

pubs.acs.org/JPCL

Constrained Excited-State Structure in Molecular Crystals by Means of the QM/MM Approach: Toward the Prediction of Photocrystallographic Results

Radosław Kamiński,*[,†,‡] Mette S. Schmøkel,[†,§] and Philip Coppens*[,†]

[†]Department of Chemistry, University at Buffalo, The State University of New York, Buffalo, New York 14260-3000, [‡]Department of Chemistry, University of Warsaw, Pasteura 1, 02-093 Warszawa, Poland, and [§]Department of Chemistry, Aarhus University, Langelandsgade 140, DK-8000 Aarhus C, Denmark

ABSTRACT The QM/MM method is applied to predict the excited triplet structure of a molecule embedded in a crystal. In agreement with experimental observation, it is found that conformation changes on excitation are severely restricted compared with geometry changes predicted for the isolated molecule. The results are of importance for understanding the photophysical properties of molecular solids.

SECTION Dynamics, Clusters, Excited States

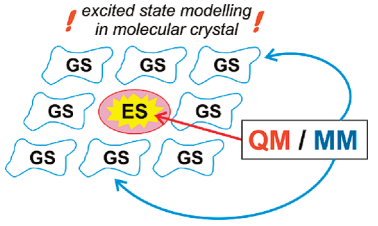

The understanding of processes occurring when matter is interacting with electromagnetic radiation is of considerable importance in modern science and engineering. Increased knowledge of such phenomena may lead to rational construction of light-sensitive devices. In order to gain appropriate insight, the nature of excited-state structures in the solid state must be evaluated. Recent advances in photocrystallographic methods now allow the determination of geometry changes upon laser irradiation in molecular crystals.[1] Although the field is still in an early stage of development because of experimental limitations and limited laser-light penetration in the crystals, considerable progress is being made as brighter X-ray sources and more advanced detectors are becoming available.

To interpret the experimental results, corresponding quantum chemical calculations are essential. However, none of the computer programs for periodic calculations are designed to deal with locally excited crystals in which the constraining effect of the environment will affect the conformation which would be attained by the excited isolated molecule. In the following, we present a quantum mechanics/molecular mechanics (QM/MM) cluster approach to simulate the light-induced molecular changes in a constraining environment.

Method. The method is based on the assumption that the population of excited molecules in the crystal is quite low (around 1−20%), as is typically the case in light-excited molecular crystals.[2] For the case of the frequently occurring random distribution of excited molecules, we assume that with one molecule in the unit cell, the excited state (**ES**) molecule in the central unit cell is surrounded by unit cells containing molecules in their ground state (**GS**). Thus, the low-percentage excitation in the solid state can be approximated by a cluster consisting of a central excited molecule surrounded by a shell of molecules in their ground state (Figure 1). This leads to populations parameters of about 11 and 4% in 2D and 3D cases, respectively. Of course, details of such molecular clusters will depend on the space group symmetry and the number of molecules in the asymmetric unit, but the principle of one excited molecule surrounded by ground-state molecules is general.

The resulting clusters may contain a few hundred atoms or more. Moreover, imposing a different spin state on such a system will lead to a delocalization of the spin density over the whole cluster, which is typically not the case in time-resolved experiments in which a nonequilibrium structure with localized excitation is examined. This problem is avoided in the QM/MM calculations,[3] in which only the central molecule is treated on the basis of quantum mechanics while the remainder of the cluster is described using a force field formalism. The static outer shell acts as a constraint in the molecular geometry optimization process. The excitation remains localized on the central molecule. It is worth noting that similar cluster QM/MM approaches have been used in the estimation of thermal motions[4] and dipole moments in molecular crystals.[5]

Computational Details. The QM/MM approach was applied to the [bis(4-chlorothiophenyl)-1,10-phenanthroline]zinc(II) complex, with the aim to compare the results with those of a parallel photocrystallographic study. Its photochemical behavior has been the subject of extensive studies by Crosby and co-workers.[6] At 35 K, ligand to ligand charge transfer (LLCT) from the thiol ligands to the phenanthroline dominates and leads to an excited triplet state with a long lifetime of about 0.13 ms.[6a] The molecule crystallizes in the monoclinic space group $P2_1/n$ with one molecule in the asymmetric unit. The zinc atom is tetrahedrally coordinated and bonded to a phenanthroline (**A**) and two chlorothiophenyl (**B**, **C**) ligands (Scheme 1). The two thiol ligands are not equivalent; one is

Received Date: June 14, 2010
Accepted Date: July 8, 2010

DOI: 10.1021/jz100809q | *J. Phys. Chem. Lett.* **2010**, *1*, 2349–2353

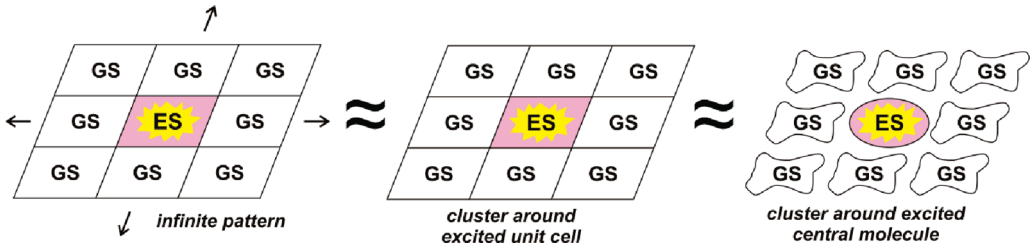

Figure 1. 2D schematic representation of the crystal environment, approximated by a molecular cluster (**GS**, ground state; **ES**, excited state).

Scheme 1. Schematic Representation of the Crystal Geometry of the Studied Complex with Selected Structural Fragments and Numbering of Crucial Atoms

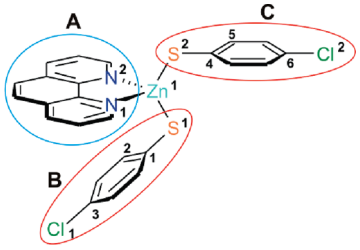

closer to the phenanthroline moiety (**B**), and the other points away from it (**C**).

On the basis of the known **GS** crystal structure, a shell of 16 molecules fully surrounding one central molecule was built. Since there are four molecules in the unit cell, this implies that the cluster does not correspond to the single unit cell description. The corresponding excited-state population parameter equals 1/17 or 5.9%. The C−H bond lengths were adjusted to the standard neutron distance of 1.083 Å.[7] The Cartesian coordinates of the cluster are listed in the Supporting Information.

Optimizations of the geometry of the central molecule were performed by means of the DFT method, as implemented in ADF program[8] (version 2009.01), using an all-electron triple-ζ STO basis with one set of polarization functions[8a] together with the zero-order regular approximation[9] (ZORA) to take into account small relativistic effects. Three functionals were tested, BP86,[10] BLYP,[10a,11] and B3LYP.[12] To evaluate the effect of the surrounding molecules, geometry optimizations were also performed for the isolated molecule using the BP86 level of theory. The Cartesian coordinates of the isolated molecules are presented in the Supporting Information. Energy minima for the isolated molecule were confirmed by calculation of vibrational frequencies within the harmonic approximation.

The AMBER force field[13] was applied in the MM part of the calculation. As the molecular shell has been fixed, only the Coulombic and dispersion forces are of importance in the simulation of the crystal environment.

Optimization of the Isolated Molecule. As the complex is very flexible, different locally stable geometries were reached upon optimization for both the **GS** and the triplet **ES**. Figure 2 shows the experimental and the two lowest-energy theoretically optimized geometries. One of the shown **GS** geometries (**1G**) closely resembles the experimental geometry in the crystal (RMSD = 0.168 Å for superimposed molecules); however, this

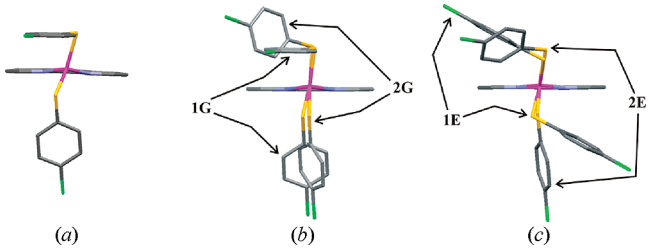

Figure 2. Example geometries (viewed approximately along the Zn to the center of the phenanthroline ligand line); (a) experimental geometry (starting point for optimizations), (b) **1G** and **2G** geometries (optimized isolated **GS**s), and (c) **1E** and **2E** geometries (optimized isolated **ES**s). Hydrogen atoms are omitted for clarity; in (b) and (c), the phenanthroline ligands of the two results are superimposed.

is not the case of the second the **2G** structure. We note that the **1G** geometry corresponds to a slightly higher energy than **2G**, the difference being about 8.02 kJ·mol^{-1}. Both **ES** geometries are very different from the **GS** crystal geometry. This is especially true for the **1E** geometry, which shows a significant change of the molecular shape upon excitation. For the purpose of comparison with the QM/MM results, only the **1G** (as it is similar to the crystal geometry) and **1E** geometries (lowest-energy structure) were considered. Selected geometrical parameters are summarized in Table 1.

Cluster Calculations. In the cluster calculations, the geometries of the **GS** and the **ES** were evaluated with all three functionals (BP86, BLYP, B3LYP), yielding six structures labeled **GSBP86** (**GS** for the BP86 functional), **ESBP86**, and so forth. In order to quantitatively compare the geometries obtained with different functionals, they were pairwise superimposed, and the root-mean-square deviations (RMSDs) between distances between corresponding atoms were calculated (Table 2). The table shows that the agreement among the different **GS** and **ES** geometries is quite reasonable. Despite the use of different exchange-correlation functionals, essentially the same results are obtained. As the geometries are similar, further conclusions are based on the BP86 geometries. Interestingly, the speed of the constrained optimizations is about as fast as or faster than that of the isolated molecule optimizations. This may be attributed to the constrained molecular geometry, which requires fewer steps to achieve acceptable geometric convergence.

Geometry Changes upon Excitation of the Constrained Molecule. The **GS** and **ES** structures are shown at their positions as fixed in the cavity in Figure 3, and selected geometrical

DOI: 10.1021/jz100809q | J. Phys. Chem. Lett. 2010, 1, 2349–2353

Table 1. Selected Geometrical Parameters for the Isolated Molecule **1G** and **1E** Structures Calculated at the BP86 Level of Theory[a]

	d/Å			α/°			τ/°	
bond	**1G**	**1E**	angle	**1G**	**1E**	torsion angle	**1G**	**1E**
Zn(1)−N(1)	2.176	2.009	N(1)−Zn(1)−N(2)	76.91	84.97	Zn(1)−S(1)−C(1)−C(2)	73.76	40.39
Zn(1)−N(2)	2.163	2.009	S(1)−Zn(1)−S(2)	122.93	84.62	Zn(1)−S(2)−C(4)−C(5)	101.75	40.39
Zn(1)−S(1)	2.253	2.359						
Zn(1)−S(2)	2.273	2.359						
S(1)−C(1)	1.789	1.760						
S(2)−C(4)	1.791	1.760						
C(3)−Cl(1)	1.767	1.757						
C(6)−Cl(2)	1.766	1.757						
S(1)···S(2)	3.976	3.176						

[a] Parameters: *d* denotes distance, α angle, and τ torsion angle.

Table 2. Root-Mean-Square Deviations (RMSDs) for Different Pairs of **GS** and **ES** Geometries of the Cluster-Embedded Molecule

geometry 1	geometry 2	RMSD/Å
GSBP86	**GSBLYP**	0.039
GSBLYP	**GSB3LYP**	0.044
GSB3LYP	**GSBP86**	0.057
ESBP86	**ESBLYP**	0.041
ESBLYP	**ESB3LYP**	0.089
ESB3LYP	**ESBP86**	0.076

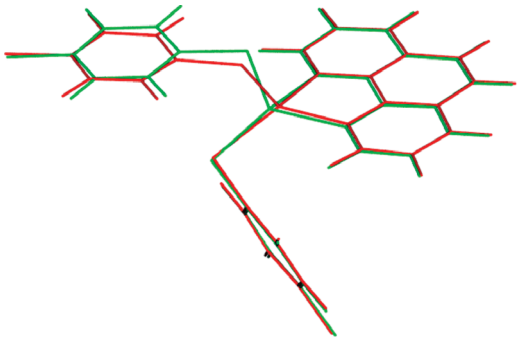

Figure 3. **GSBP86** (green) and **ESBP86** (red) geometries as located in the crystal cavity.

parameters are listed in Table 3. Significant shifts of the atoms are evident. The Zn−N bonds are shortened by about 0.16 Å upon excitation, whereas the N−Zn−N angle increases by about 7°. This results from a slight movement of the zinc atom toward the phenanthroline ligand. Significant differences are also observed for Zn−S bonds, which show an average elongation of about 0.08 Å. The S−Zn−S angle decreases by about 8.5°, corresponding to a significant shortening of the S···S distance from about 3.9 to 3.7 Å. A slight decrease of the S−C and C−Cl bonds suggests that the phenyl rings exhibit a more quinone-like structure in the excited state. Interestingly, the torsion angles indicate a slight rotation of the **B** and **C** ligands along the S−C bonds. Also, both ligands are clearly not equivalent as the shift of the S(2) atom is much larger than that of S(1) (about 0.43 and 0.11 Å, respectively).

The possibility of weak S···S bonding in the excited state is not well-established as the distance remains larger than 3.6 Å, which is the sum of the van der Waals radii.[14] On the other hand, such bond formation is supported by the calculated bond orders. For the **GSBP86**, the Mayer[15] and Nalewajski-Mrozek[16] bond orders are equal to 0.001 and 0.097, respectively, compared with 0.093 and 0.186 for the excited state, **ESBP86**.

Effect of the Cavity on the Excited-State Geometry. A striking difference between the geometry of the excited state of the isolated molecule and that in the cavity is evident from the S···S distances. In the isolated molecule, this distance decreases by 0.80 Å upon excitation, whereas according to the calculation in the cavity, the change is much less pronounced at 0.29 Å. This is illustrated in Figure 4, in which the phenanthroline ligands in the two structures have been superimposed. It is clear that the thiol ligands point in completely different directions in the two cases. The results of the cavity calculation indicate that the large shift of the thiol ligands is impeded by the surrounding molecules. This is in agreement with the reduced change in conformation upon excitation of molecules in crystals surmised previously by Highland et al.[6a] and also observed in earlier photocrystallographic experiments on a copper(I) phenanthroline photosensitizer dye.[17]

In summary, the QM/MM method presented above leads to the prediction of atomic shifts resulting from photoexcitation of molecules embedded in crystals and is therefore of particular importance for comparison with photocrystallographic results. It is found in the example examined that the geometry of the excited molecule differs considerably from that obtained from isolated molecule calculations. The QM/MM approach can be extended to evaluate electronic properties of molecules in crystals, including the electron density distribution.

SUPPORTING INFORMATION AVAILABLE Cartesian coordinates of the calculated isolated molecular structures at the BP86 level. Cartesian coordinates of the ground- and excited-state central molecules in the cluster at the BP86, B3LYP, and BLYP levels. Geometry of the cluster and Cartesian coordinates of the experimental ground-state molecular structure. This material is available free of charge via the Internet at http://pubs.acs.org.

DOI: 10.1021/jz100809q | *J. Phys. Chem. Lett.* **2010**, *1*, 2349–2353

Table 3. Selected Geometrical Parameters for **GS** and **ES** Structures Calculated at the BP86 Level of Theory in the Crystal Cavity[a]

	d/Å			α/°			τ/°	
bond	GSBP86	ESBP86	angle	GSBP86	ESBP86	torsion angle	GSBP86	ESBP86
Zn(1)−N(1)	2.157	2.008	N(1)−Zn(1)−N(2)	76.96	84.35	Zn(1)−S(1)−C(1)−C(2)	67.58	68.66
Zn(1)−N(2)	2.169	2.018	S(1)−Zn(1)−S(2)	121.69	103.14	Zn(1)−S(2)−C(4)−C(5)	104.72	123.47
Zn(1)−S(1)	2.252	2.329						
Zn(1)−S(2)	2.264	2.338						
S(1)−C(1)	1.786	1.762						
S(2)−C(4)	1.788	1.751						
C(3)−Cl(1)	1.764	1.753						
C(6)−Cl(2)	1.761	1.748						
S(1)···S(2)	3.944	3.656						

[a] Parameters: *d* denotes distance, α angle, and τ torsion angle.

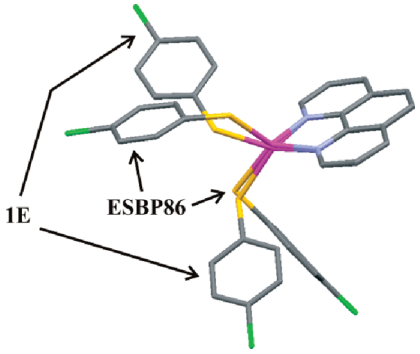

Figure 4. Comparison of **1E** (excited state of the isolated molecule) and **ESBP86** (the constrained QM/MM optimization) geometries. The phenanthroline ligands are superimposed.

AUTHOR INFORMATION

Corresponding Author:

*To whom correspondence should be addressed. E-mail: rkaminski@chem.uw.edu.pl (R.K.); coppens@buffalo.edu (P.C.).

ACKNOWLEDGMENT This research has been supported by the U.S. National Science Foundation (CHE0843922). The authors thank Jason B. Benedict for helpful discussions and Derek M. Peloquin for some of the early calculations. R.K. would like to thank the Foundation for Polish Science for financial support within the International PhD Projects program. M.S.S. is grateful to the Danish National Research Foundation and the Danish Strategic Research Council for financial support.

REFERENCES

(1) (a) Woike, T., Schaniel, D., Eds. Photocrystallography. *Z. Kristallogr.* **2008**, *223*. (b) Collet, E., Ed. Dynamical Structural Science. *Acta Crystallogr., Sect. A* **2010**, *66*.

(2) Coppens, P.; Benedict, J. B.; Messerschmidt, M.; Novozhilova, I.; Graber, T.; Chen, Y.-S.; Vorontsov, I.; Scheins, S.; Zheng, S.-L. Time-Resolved Synchrotron Diffraction and Theoretical Studies of Very Short-Lived Photo-Induced Molecular Species. *Acta Crystallogr., Sect. A* **2010,** *66*, 179–188.

(3) (a) Svensson, M.; Humbel, S.; Froese, R. D. J.; Matsubara, T.; Sieber, S.; Morokuma, K. ONIOM: A Multilayered Integrated MO + MM Method for Geometry Optimizations and Single Point Energy Predictions. A Test for Diels−Alder Reactions and Pt(P(*t*-Bu)$_3$)$_2$ + H$_2$ Oxidative Sddition. *J. Phys. Chem.* **1996**, *100*, 19357−19363, and references therein. (b) Woo, T. K.; Cavallo, L.; Ziegler, T. Implementation of the IMOMM Methodology for Performing Combined QM/MM Molecular Dynamics Simulations and Frequency Calculations. *Theor. Chem. Acc.* **1998**, *100*, 307, and references therein.

(4) Dittrich, B. 16th Sagamore Conference, Santa Fe, NM, 2009.

(5) Whitten, A. E.; Spackman, M. A. Anisotropic Displacement Parameters for H Atoms Using an ONIOM Approach. *Acta Crystallogr., Sect. B* **2006,** *62*, 875–888.

(6) (a) Highland, R. C.; Brummer, J. G.; Crosby, G. A. Redistribution of Excitation Energy between Nonequilibrated Electronic Excited Levels of Zinc(II) Complexes. *J. Phys. Chem.* **1986,** *90*, 1593–1598. (b) Highland, R. G.; Crosby, G. A. Determination of the Activation Barrier to Energy Transfer from $^3\pi\pi^*$ to Charge Transfer Levels via Steady-State and Transient Luminescence Measurements on Bis(4-chlorothiophenol)(1,10-phenanthroline)zinc(II). *Chem. Phys. Lett.* **1985,** *119*, 454–458. (c) Truesdell, K. A.; Crosby, G. A. Observation of a Novel Low-Lying Excited State in Zinc(II) Complexes. *J. Am. Chem. Soc.* **2002,** *107*, 1787–1788.

(7) (a) Allen, F. H.; Bruno, I. J. Bond Lengths in Organic and Metal-Organic Compounds Revisited: X−H Bond Lengths from Neutron Diffraction Data. *Acta Crystallogr., Sect. B* **2010,** *66*, 380–386. (b) Allen, F. H.; Kennard, O.; Watson, D. G.; Brammer, L.; Orpen, A. G.; Taylor, R. Tables of Bond Lengths Determined by X-ray and Neutron Diffraction. Part I. Bond Lengths in Organic Compounds. *J. Chem. Soc., Perkin Trans. II* **1987,** *2*, S1–S19.

(8) (a) *ADF, 2009.01*; SCM, Theoretical Chemistry, Vrije Universiteit: Amsterdam, The Netherlands, 2009. (b) Guerra, C. F.; Snijders, J. G.; Velde, G. t.; Baerends, E. J. Towards an Order-N DFT Method. *Theor. Chem. Acc.* **1998,** *99*, 391–403. (c) Velde, G. t.; Bickelhaupt, F. M.; Baerends, E. J.; Guerra, F.; Gisbergen, S. J. A. v.; Snijders, J. G.; Ziegler, T. Chemistry with ADF. *J. Comput. Chem.* **2001,** *22*, 931–967.

(9) (a) Lenthe, E. v.; Baerends, E. J.; Snijders, J. G. Relativistic Regular Two-Component Hamiltonians. *J. Chem. Phys.* **1993,** *99*, 4597. (b) Lenthe, E. v.; Baerends, E. J.; Snijders, J. G. Relativistic Total Energy Using Regular Approximations. *J. Chem. Phys.* **1994,** *101*, 9783. (c) Lenthe, E. v.; Ehlers, A. E.; Baerends, E. J. Geometry Optimization in the Zero Order Regular Approximation for Relativistic Effects. *J. Chem. Phys.* **1999,** *110*, 8943. (d) Lenthe, E. v.; Leeuwen, R. v.; Baerends, E. J.; Snijders, J. G. Relativistic Regular Two-Component

DOI: 10.1021/jz100809q | *J. Phys. Chem. Lett.* **2010**, *1*, 2349–2353

Hamiltonians. *Int. J. Quantum Chem.* **1996,** *57*, 281. (e) Lenthe, E. v.; Snijders, J. G.; Baerends, E. J. The Zero-Order Regular Approximation for Relativistic Effects: The Effect of Spin-Orbit Coupling in Closed Shell Molecules. *J. Chem. Phys.* **1996,** *105*, 105.

(10) (a) Becke, A. D. Density-Functional Exchange-Energy Approximation with Correct Asymptotic Behavior. *Phys. Rev. A* **1988,** *38*, 3098. (b) Perdew, J. P. Density-Functional Approximation for the Correlation Energy of the Inhomogeneous Electron Gas. *Phys. Rev. B* **1986,** *33*, 8822. (c) Perdew, J. P. Erratum to: Density-Functional Approximation for the Correlation Energy of the Inhomogeneous Electron Gas. *Phys. Rev. B* **1986,** *34*, 7406.

(11) (a) Johnson, B. G.; Gill, P. M. W.; Pople, J. A. The Performance of a Family of Density Functional Methods. *J. Chem. Phys.* **1993,** *98*, 5612. (b) Lee, C.; Yang, W.; Parr, R. G. Development of the Colle−Salvetti Correlation-Energy Formula into a Functional of the Electron Density. *Phys. Rev. B* **1988,** *37*, 785. (c) Russo, T. V.; Martin, R. L.; Hay, P. J. Density Functional Calculations on First-Row Transition Metals. *J. Chem. Phys.* **1994,** *101*, 7729.

(12) Stephens, P. J.; Devlin, F. J.; Chabalowski, C. F.; Frisch, M. J. Ab Initio Calculation of Vibrational Absorption and Circular Dichroism Spectra Using Sensity Functional Force Fields. *J. Phys. Chem.* **1994,** *98*, 11623.

(13) Cornell, W. D.; Cieplak, P.; Bayly, C. I.; Gould, I. R.; K., M. M., Jr.; Ferguson, D. M.; Spellmeyer, D. C.; Fox, T.; Caldwell, J. W.; Kollman, P. A. A Second Generation Force Field for the Simulation of Proteins, Nucleic Acids, And Organic Molecules. *J. Am. Chem. Soc.* **1995,** *117*, 5179–5197.

(14) Bondi, A. van der Waals Volumes and Radii. *J. Phys. Chem.* **1964,** *68*, 441–51.

(15) (a) Bridgeman, A. J.; Cavigliasso, G.; Ireland, L. R.; Rothery, J. The Mayer Bond Order as a Tool in Inorganic Chemistry. *J. Chem. Soc., Dalton Trans.* **2001,** 2095–2108. (b) Mayer, I. Charge, Bond Order and Valence in the Ab Initio SCF Theory. *Chem. Phys. Lett.* **1983,** *97*, 270–274. (c) Mayer, I. Bond Order and Valence: Relations to Mulliken'S Population Analysis. *Int. J. Quantum Chem.* **1984,** *26*, 151–154.

(16) (a) Michalak, A.; DeKock, R. L.; Ziegler, T. Bond Multiplicity in Transition-Metal Complexes: Applications of Two-Electron Valence Indices. *J. Phys. Chem. A* **2008,** *112*, 7256–7263. (b) Nalewajski, R. F.; Mrozek, J. Modified Valence Indices from the Two-Particle Density Matrix. *Int. J. Quantum Chem.* **1994,** *51*, 187–200. (c) Nalewajski, R. F.; Mrozek, J.; Michalak, A. Two-Electron Valence Indices from the Kohn−Sham Orbitals. *Int. J. Quantum Chem.* **1997,** *61*, 589–601.

(17) Vorontsov, I. I.; Graber, T.; Kovalevsky, A. Y.; Novozhilova, I. V.; Gembicky, M.; Chen, Y.-S.; Coppens, P. Capturing and Analyzing the Excited-State Structure of a Cu(I) Phenanthroline Complex by Time-Resolved Diffraction and Theoretical Calculations. *J. Am. Chem. Soc.* **2009,** *131*, 6566–6573.

DOI: 10.1021/jz100809q | *J. Phys. Chem. Lett.* **2010,** *1*, 2349–2353